

A. Boudia, S. Messalti, S. Zeghlache, A. Harrag

Type-2 fuzzy logic controller-based maximum power point tracking for photovoltaic system

Introduction. Photovoltaic (PV) systems play a crucial role in converting solar energy into electricity, but their efficiency is highly influenced by environmental factors such as irradiance and temperature. To optimize power output, Maximum Power Point Tracking (MPPT) techniques are used. This paper introduces a novel approach utilizing a Type-2 Fuzzy Logic Controller (T2FLC) for MPPT in PV systems. The **novelty** of the proposed work lies in the development of a T2FLC that offers enhanced adaptability by managing a higher degree of uncertainty, we introduce an original method that calculates the error between the output voltage and a dynamically derived reference voltage, which is obtained using a mathematical equation. This reference voltage adjusts in real-time based on changes in environmental conditions, allowing for more precise and stable MPPT performance. The **purpose** of this paper is to design and validate the effectiveness of a T2FLC-based MPPT technique for PV systems. This approach seeks to enhance power extraction efficiency in response to dynamic environmental factors such as changing irradiance and temperature. The **methods** used in this study involve the implementation of T2FLC to adjust the duty cycle of a DC-DC converter for continuous and precise MPPT. The system was simulated under various environmental conditions, comparing the performance of T2FLC against T1FLC. The **results** show that the T2FLC MPPT system significantly outperforms traditional methods in terms of tracking speed, stability, and power efficiency. T2FLC demonstrated faster convergence to the MPP, reduced oscillations, and higher accuracy in rapidly changing environmental conditions. The findings of this study confirm the **practical value** of T2FLC logic in improving the efficiency and stability of PV systems, making it a promising solution for enhancing renewable energy technologies. References 33, tables 4, figures 10.

Key words: fuzzy logic controller, DC-DC boost converter, maximum power point tracking, photovoltaic system.

Вступ. Фотоелектричні (PV) системи відіграють вирішальну роль у перетворенні сонячної енергії в електрику, але їхня ефективність сильно залежить від факторів навколишнього середовища, таких як освітленість та температура. Для оптимізації вихідної потужності використовують методи відстеження точки максимальної потужності (MPPT). У цій статті наведено новий підхід з використанням контролера нечіткої логіки типу 2 (T2FLC) для MPPT у PV системах. **Новизна** запропонованої роботи полягає у розробці T2FLC, який забезпечує покращену адаптивність за рахунок управління вищим ступенем невизначеності; ми представляємо оригінальний метод, який обчислює помилку між вихідною напругою та динамічно отриманою опорною напругою, яка виходить за допомогою математичного рівняння. Ця опорна напруга регулюється в режимі реального часу на основі змін умов довкілля, що дозволяє забезпечити більш точну та стабільну роботу MPPT. **Метою** статті є розробка та перевірка ефективності методу MPPT на основі T2FLC для PV систем. Цей підхід спрямований на підвищення ефективності отримання енергії у відповідь на динамічні фактори навколишнього середовища, такі як зміна освітленості та температури. **Методи**, що використовуються у цьому дослідженні, включають реалізацію T2FLC для регулювання робочого циклу DC-DC-перетворювача для безперервного та точного MPPT. Система була змодельована у різних умовах навколишнього середовища, порівнюючи продуктивність T2FLC та T1FLC. **Результати** показують, що система MPPT T2FLC значно перевершує традиційні методи з погляду швидкості відстеження, стабільності та енергоефективності. T2FLC продемонструвала більш швидку збіжність до MPP, зменшені коливання та більш високу точність у швидко мінливих умовах довкілля. Результати цього дослідження підтверджують **практичну цінність** логіки T2FLC для підвищення ефективності та стабільності PV систем, що робить її перспективним рішенням для покращення технологій відновлюваної енергії. Бібл. 33, табл. 4, рис. 10.

Ключові слова: контролер нечіткої логіки, DC-DC підвищувальний перетворювач, відстеження точки максимальної потужності, фотоелектрична система.

Introduction. Photovoltaic (PV) systems have garnered considerable interest as a viable and renewable energy source. The efficiency of these systems largely depends on the ability to maximize the extraction of electrical power from solar panels, a process known as Maximum Power Point Tracking (MPPT). The PV module output power is highly sensitive to environmental conditions changes, making the MPPT a critical component in PV systems [1–4].

Traditional MPPT methods, including Incremental Conductance (IC), Perturb and Observe (P&O) [3, 5, 6] have been extensively utilized due to their straightforwardness and effortless integration. However, these methods often exhibit limitations in dynamic environments [7]. For instance, the P&O method may exhibit oscillations around the Maximum Power Point (MPP) under stable conditions and fail to track the MPP accurately during rapidly changing conditions. The IC method, while more accurate, can be computationally intensive and slow in response [8–10].

Advanced MPPT techniques have been developed to address these challenges [11, 12], among which are Fuzzy Logic Controllers (FLCs) [13], which have shown promise. Based on fuzzy logic theory, FLC can handle the nonlinear and uncertain nature of PV systems more effectively than traditional methods. By mimicking human reasoning and

decision-making processes, FLC can provide a more robust and adaptive approach to MPPT [14].

Type-1 FLCs (T1FLCs) have been successfully applied to MPPT [15], demonstrating improved performance over conventional methods [16]. However, T1FLCs have limitations in dealing with uncertainties and imprecise information, which are inherent in PV systems. This has led to the development of Type-2 FLCs (T2FLCs), which offer an enhanced capability to manage uncertainties by introducing a higher degree of fuzziness.

The implementation of T2FLCs in MPPT for PV systems has emerged as a promising approach to enhance the efficiency and reliability of solar energy systems [17]. The inherent nonlinear characteristics of PV systems, influenced by environmental factors such as temperature and irradiance, necessitate advanced control strategies that can adapt to these variations. Type-2 fuzzy logic, an extension of traditional fuzzy logic, provides a robust framework for handling uncertainty and imprecision in the control process, making it particularly suitable for MPPT applications. T2FLCs are designed to manage the complexities associated with the nonlinear output of PV systems. As highlighted by the application of Type-2 fuzzy logic in MPPT allows for improved performance in environments with high uncertainty, such as varying

weather conditions [18, 19]. This is crucial since the output power of PV systems is not only dependent on solar irradiance but also on temperature fluctuations, which can affect the efficiency of energy conversion. The ability of Type-2 fuzzy logic to incorporate degrees of uncertainty in its decision-making process enables it to adapt more effectively to these dynamic changes compared to traditional T1FLCs [18].

The performance of T2FLCs in MPPT has been demonstrated through various studies. For instance, a novel algorithm utilizing a T2FLC in conjunction with a push-pull converter developed, showing significant improvements in tracking efficiency and total harmonic distortion reduction [20]. This aligns with findings from who proposed an asymmetrical fuzzy logic control-based MPPT algorithm that simplified calculations while enhancing both dynamic and steady-state performance [21]. The results indicate that Type-2 fuzzy logic not only improves the tracking speed but also stabilizes the output power under fluctuating conditions, which is essential for maximizing energy yield from PV systems.

Moreover, the integration of T2FLCs with dual-axis solar tracking systems further enhances the effectiveness of MPPT strategies. It is demonstrated that combining Type-2 fuzzy logic with a photo-resistive tracking method significantly improved the power output of solar trackers, showcasing the synergy between advanced control strategies and tracking technologies [18]. This combination allows for continuous adjustment of the PV panels' orientation, ensuring optimal exposure to sunlight throughout the day, thereby maximizing energy capture.

Furthermore, the integration of Type-2 fuzzy logic with other control strategies, such as ANFIS, has shown promising results in enhancing MPPT performance. Compared fuzzy logic and ANFIS-based MPPT controllers, revealing that the hybrid approach could leverage the strengths of both methodologies to improve tracking accuracy and efficiency [19]. This suggests that the future of MPPT in PV systems may lie in the combination of multiple intelligent control strategies to address the challenges posed by environmental variability.

The ongoing research into T2FLCs for MPPT continues to yield innovative solutions that enhance the efficiency and reliability of PV [20]. As the demand for renewable energy sources grows, the development of advanced control strategies that can adapt to changing conditions will be crucial in maximizing the potential of solar energy. The findings from various studies underscore the importance of Type-2 fuzzy logic in achieving optimal performance in MPPT applications, paving the way for more efficient and sustainable energy systems.

The aim of the paper is to develop and demonstrate the effectiveness of a T2FLC-based MPPT technique for PV systems. The goal is to improve power extraction efficiency under varying environmental conditions, such as fluctuating irradiance and temperature, by addressing the limitations of in T1FLCs. The paper seeks to highlight how the adaptive capabilities of the T2FLC can enhance tracking speed, reduce oscillations, and improve overall accuracy, ultimately contributing to the optimization of PV system performance and efficiency.

The primary distinction between our work and previous studies lies in the method used to implement the fuzzy logic control for MPPT in PV systems. In our approach, we introduce an original method that calculates

the error between the output voltage and a reference voltage. Which is calculated by mathematic equation, this equation provides a precise value that dynamically adjusts according to variations in irradiance and temperature. By employing this mathematical model, the system is capable of calculating an accurate reference voltage, ensuring more precise and stable MPPT performance even under fluctuating environmental conditions. In contrast, many previous studies employ a more conventional approach to fuzzy logic control, often modifying the P&O algorithm by replacing its decision-making process with fuzzy logic [17, 21–24]. These approaches, which are commonly applied in both Type-1 and Type-2 fuzzy logic control, focus primarily on improving the efficiency of P&O by mitigating oscillations and improving response times [25–27]. However, these methods are limited by their reliance on fixed reference points or simplified control rules, which can reduce their effectiveness in highly dynamic environments. Our method's ability to generate a real-time, dynamically adjusted reference voltage offers a significant improvement in tracking accuracy and system stability.

PV system modelling. PV cell, also known as a solar cell, is the basic unit in a PV that converts sunlight directly into electrical energy through the PV effect. When sunlight (photons) hits the PV cell, it can excite electrons in the semiconductor material, creating free electrons (negative charge) and holes (positive charge).

The electric field at the P-N junction separates these charges, causing them to move in opposite directions and generate an electric current when connected to a load [5]. The single-diode model of a PV cell is expressed as:

$$I = I_{ph} - \frac{I_0}{e^{(V+IR_S)/nV_t} - 1} - \frac{V + IR_S}{nV_t}, \quad (1)$$

where I is the output current; I_{ph} is the photocurrent; I_0 is the reverse saturation current; V is the terminal voltage; R_s is the series resistance; R_{sh} is the shunt resistance; n is the ideality factor; V_t is the thermal voltage.

Figure 1 illustrates the performance of a PV BP SX 60 system under varying temperature and irradiance conditions, with fuzzy logic Type-2 employed for MPPT, it demonstrates the influence of irradiation on the cell at a constant temperature (a) and the impact of temperature on the cell with a set level of irradiation (b).

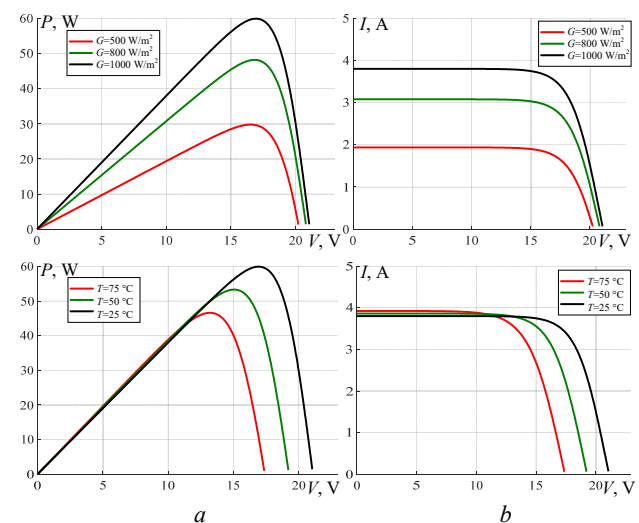


Fig. 1. The characteristics of $P(V)$ (a) and $I(V)$ (b) fluctuate with variations in environmental factors such as irradiation G and temperature T

Temperature impact.

• *I-V* curve: The *I-V* relationship at different temperatures: 25 °C, 50 °C, 75 °C demonstrates that as the temperature increases, the voltage decreases significantly which is typical behavior for PV cells. The current slightly increases with higher temperatures, but the overall power decreases due to the reduction in voltage.

• *P-V* curve: The *P-V* relationship shows that with increasing temperature (moving from black to red), the MPP shifts to a lower voltage and reduces in magnitude. The PV system loses efficiency as temperature increases, which is evident in the shift and reduction of the power output at 75 °C compared to 25 °C.

Irradiance impact.

• *I-V* curve: the *I-V* curve illustrates the effect of irradiance levels (500 W/m², 800 W/m², 1000 W/m²). As irradiance increases, both the current and voltage increase, improving the power output. The *I-V* curve shows that at higher irradiance (black line), the current significantly increases, which leads to a larger area under the curve, indicating more power generation.

• *P-V* curve: The *P-V* curve demonstrates the relationship between power and voltage under different irradiance conditions. As irradiance increases, the power output increases significantly, and the MPP shifts upwards. The PV system performs better at higher irradiance levels, with the MPP for 1000 W/m² being much higher than that for 500 W/m².

Type-2 fuzzy logic control. Fuzzy logic Type-2 and Type-1 display notable resemblances. However, there are two basic differences between them, specifically, the forms of the function membership and the output of the processor. The interval of Type-2 fuzzy logic control comprises multiple components, including a fuzzifier, an inference engine, type reduction, rule bases and a defuzzifier. This section offers a concise summary of the main characteristics of T2FLC and introduces important ideas associated with them [28].

Functions membership. T2FLC is distinguished by the configuration of their function membership. Figure 2 shows two distinct functions of membership: *a* – standard T1FLC membership function; *b* – fuzzy Type-1 functions membership that depicts a blurred representation Type-2 functions membership refers to a specific type of mathematical function used in fuzzy logic systems [29].

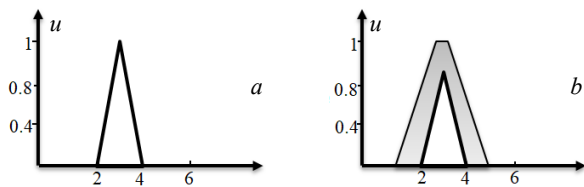


Fig. 2. Type-1 functions membership (a) and uncertainty footprint (b)

Definition 1. T2FLC system, represented as \tilde{A} , is defined by a functions membership Type-2 $\mu_{\tilde{A}} = (x, \mu)$, with $x \in X$ and $\mu \in J_x \subseteq [0, 1]$:

$$\tilde{A} = \{(x, u), \mu_{\tilde{A}}(x, u)\} \mid \forall x \in X, \forall u \in J_x \subseteq [0, 1]. \quad (2)$$

Type-2 function membership is a bivariate function that is contingent upon two variables, x and u . It is

important to mention that $\mu_{\tilde{A}} = (x, \mu)$ is a value that falls within the range of 0 to 1 [30]:

$$\tilde{A} = \int_{x \in X} \int_{u \in J_x} \mu_{\tilde{A}}(x, u) / (x, u) J_x \subseteq [0, 1], \quad (3)$$

where the symbol \int represents the union of all x and u .

Definition 2. \tilde{A} is an interval T2FLC system where the function membership $\mu_{\tilde{A}}(x, \mu)$ is equal to 1 for all values of x and u [31].

Definition 3. The primary function membership of x refers to the scope of a secondary function membership. Thus, J_x represents the main membership of x . By employing this notation, the equation (3) can be restated as:

$$\tilde{A} = \{(x, u), \mu_{\tilde{A}}(x, u)\} \mid \forall x \in X. \quad (4)$$

Footprint of Uncertainty is the crucial parameter in T2FLC and is commonly employed in this paper. This term represents the ambiguity inside the system, providing a practical way to describe the complete range of the secondary function membership.

Definition 4. The uncertainty in the primary memberships of T2FLC is represented by a confined region referred to as the Fuzzy Output Universe (FOU). This region is the primary union of all function memberships [31], i.e.:

$$FOU(\tilde{A}) = U_{x \in X} / J_x. \quad (5)$$

Definition 5. When the FOU of a T2FLC is constrained by two Type-1 functions membership, the upper function membership corresponds to the upper bound, denoted by $\overline{\mu_{\tilde{A}}}(x), \forall x \in X$, and the lower function membership corresponds to the lower bound, noted by $\underline{\mu_{\tilde{A}}}(x), \forall x \in X$. This relationship can be expressed as [32]:

$$\begin{aligned} \overline{\mu_{\tilde{A}}} &= \overline{FOU(\tilde{A})}, \forall x \in X \\ \underline{\mu_{\tilde{A}}} &= \underline{FOU(\tilde{A})}, \forall x \in X. \end{aligned} \quad (6)$$

Definition 6. An embedded Type-2 set \tilde{A}_e is provided for a continuous universe of discourse X and U [31]:

$$\tilde{A}_e = \int_{x \in X} [f_x(\theta / \theta)] / x \dots \theta \in J_x \subseteq [0, 1]. \quad (7)$$

The set \tilde{A}_e is a subset of set \tilde{A} , and there exist an unlimited number of Type-2 sets.

T2FLC structure. Figure 3 illustrates the structure general of a T2FLC. This structure resembles that of a T1FLC, with the primary difference being the output processor. The output processor comprises two processes: type-reduction and defuzzification. The following sections will explain each component of Fig. 3 in detail.

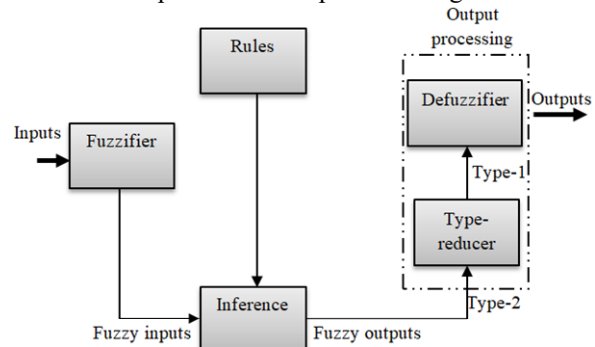


Fig. 3. Structure of T2FLC [31]

Fuzzifier. The initial block in Fig. 3 is the Fuzzifier, which converts the precise inputs into fuzzy values. The fuzzifier transforms the precise input vector $x^T = (x_1, x_2, \dots, x_n)^T$ into a Type-2 fuzzy system \tilde{A}_x , using a similar process as in a Type-1 fuzzy logic system.

Rules. The i -th rule in a Type-2 fuzzy logic system can be represented in the following generic form:

If x_1 is \tilde{F}_1^i and x_2 is \tilde{F}_2^i and ... x_n is \tilde{F}_n^i .

Then:

$$y^i = \tilde{G}^i, \quad (8)$$

where $i = 1, \dots, M$; \tilde{F}_j^i represents the T2FLC for the input state j of the i -th rule, x_1, x_2, \dots, x_n are the inputs, \tilde{G}^i is the output of Type-2 fuzzy system for rule i , and M is the total number of rules. As can be seen, the rule structure of a T2FLC is almost identical to that of a Type-1, with the only difference being the replacement of Type-1 functions membership with their Type-2 equivalents.

Inference engine. In fuzzy system interval Type-2 using the minimum or product t -norm operations, the i -th activated rule is processed $F^i = (x_1, \dots, x_n)$ gives us the interval that is determined by two extreme:

$$\begin{aligned} \underline{f}^i &= (x_1, \dots, x_n) \quad \text{and} \quad \bar{f}^i = (x_1, \dots, x_n) \quad [33]; \\ F^i &= (x_1, \dots, x_n) = \\ &= \left[\underline{f}^i = (x_1, \dots, x_n), \bar{f}^i = (x_1, \dots, x_n) \right] \equiv \left[\underline{f}^i, \bar{f}^i \right], \quad (9) \end{aligned}$$

where \underline{f}^i and \bar{f}^i are:

$$\begin{aligned} \underline{f}^i &= \underline{\mu}_{F_1^i}(x_1) \times \dots \times \underline{\mu}_{F_n^i}(x_n); \\ \bar{f}^i &= \bar{\mu}_{F_1^i}(x_1) \times \dots \times \bar{\mu}_{F_n^i}(x_n). \end{aligned} \quad (10)$$

Type reducer. T2FLC is calculated after the rules are triggered and inference is performed, resulting in a Type-1 fuzzy system. This section explores the techniques for calculating the centroid of a T2FLC using the extension concept [31]. The centroid of a Type-1 fuzzy system A can be mathematically represented as:

$$C_A = \frac{\sum_{i=1}^n z_i w_i}{\sum_{i=1}^n w_i}, \quad (11)$$

where n is the number of discretized domains of A , $z_i \in R$ and $W_i \in [0, 1]$.

If each z_i and w_i are replaced with a Type-1 fuzzy systems, Z_i and W_i , having associated functions membership of $\mu_z(z_i)$ and $\mu_w(W_i)$ respectively, then by applying the extension principle, the generalized centroid for the Type-2 fuzzy \tilde{A} is given by:

$$GC_{\tilde{A}} = \int \dots \int \int \dots \int \frac{\left[T_{i=1}^n \mu_z(z_i) \cdot T_{i=1}^n \mu_w(z_i) \right]}{\sum_{i=1}^n z_i w_i / \sum_{i=1}^n w_i}, \quad (12)$$

where T is the t -norm; note that $GC_{\tilde{A}}$ is T1FLC. For interval of T2FLC:

$$GC_{\tilde{A}} = \int \dots \int \int \dots \int 1 / \frac{\sum_{i=1}^n z_i w_i}{\sum_{i=1}^n w_i} = [y_l, y_r]. \quad (13)$$

Karnik–Mendel algorithms. The well-known Karnik–Mendel techniques are used to determine the

centroid of interval T2FLC, the most widely used Type-2 system. Initially, the expression (13) is written as:

$$f^M \in \left[\underline{f}^M, \bar{f}^M \right] \quad \frac{\int \sum_{i=1}^M f^i y^i}{\sum_{i=1}^M f^i}. \quad (14)$$

Iterative techniques are provided by the algorithms of Karnik–Mendel to calculate y_l, y_r in (14) as follows.

To calculate y_r :

1. For the sake of simplicity, let's assume that the values of y_{ri} are sorted in ascending order; i.e. $y_r^1 \leq y_r^2 \leq \dots \leq y_r^M$

2. Compute y_r as $y_r = \frac{\sum_{i=1}^M f_r^i y_r^i}{\sum_{i=1}^M f_r^i}$ by initially

setting $f_r^i = \frac{f^i + \bar{f}^i}{2}$ for $i = 1, \dots, M$ and let $y_r' \equiv y_r$.

3. Locate R ($1 \leq R \leq M-1$) such that $y_r^R \leq y_r' \leq y_r^{R+1}$

4. Compute $y_r = \frac{\sum_{i=1}^M f_r^i y_r^i}{\sum_{i=1}^M f_r^i}$ with $f_r^i = \underline{f}^i$

for $i \leq R$ and $f_r^i = \bar{f}^i$ for $i > R$ and let $y_r'' \equiv y_r$.

5. If $y_r'' \neq y_r'$, then go to step 6. If $y_r'' = y_r'$, then stop and set $y_r'' \equiv y_r$.

6. Return to step 3 after setting equal to y_r'' .

The process of calculating y_l is highly analogous to that of computing y_r . Simply substitute y_r^i with y_l^i in step 3, find L ($1 \leq L \leq M-1$) such that In step 2, calculate y_l as

$$y_l = \frac{\sum_{i=1}^M f_l^i y_l^i}{\sum_{i=1}^M f_l^i} \quad \text{by initially setting } f_l^i = \frac{f^i + \bar{f}^i}{2}$$

for $i = 1, \dots, M$ and in step 4, calculate $y_l = \frac{\sum_{i=1}^M f_l^i y_l^i}{\sum_{i=1}^M f_l^i}$

with $f_l^i = \bar{f}^i$ for $i \leq L$ and $f_l^i = \underline{f}^i$ for $i \geq L$.

Defuzzifier. In order to achieve a clear and precise output from a T1FLC, it is necessary to defuzzify the type-reduced set. A widely used approach is to determine the centroid of the set after reducing its type. The centroid of the discretized set Y , consisting of m points, is determined as follows:

$$y_{output}(x) = \frac{\sum_{i=1}^m y^i \mu(y^i)}{\sum_{i=1}^m \mu(y^i)}. \quad (15)$$

The output is calculated using the algorithms of iterative Karnik–Mendel, which leads to the defuzzified output of an interval T2FLC:

$$y_{output}(x) = \frac{y_l(x) + y_r(x)}{2}. \quad (16)$$

Simulation studies. The fundamental structure of the system depicted in Fig. 4 is outlined as follows. To optimize the power output, a mathematical model is employed to calculate the reference voltage V_{ref} , which is dynamically adjusted based on environmental factors such as irradiance G and temperature T :

$$V_{ref} = \frac{N_S \cdot n \cdot k \cdot T}{q} \log\left(\frac{I_{ph} - I_{ref} + I_0}{I_0}\right), \quad (17)$$

where N_S is the number of cells in series; n is the diode's ideality factor; k is the Boltzmann constant; q is the charge of the electron; T is the absolute temperature of the p - n junction; I_{ref} is the reference current.

MPPT is implemented using a T2FLC, which determines the optimal operating point of the PV system. The boost converter then adjusts the output voltage to match the calculated V_{ref} , ensuring that the system operates at maximum efficiency.

Simulation results are conducted utilizing the BP SX 60 PV module, which is widely recognized for its reliability in solar energy applications. Figure 4 illustrates the overall PV system architecture employing the T2FLC for MPPT, showcasing the integration of the PV module, the FLC and the DC-DC boost converter.

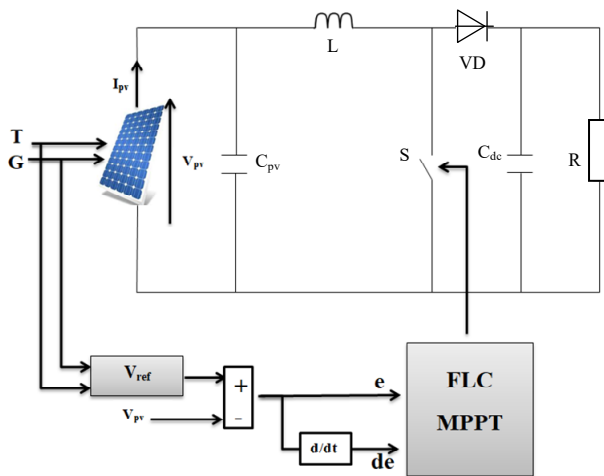


Fig. 4. PV system with FLC MPPT

The detailed parameters of the DC-DC boost converter are provided in Table 1. The simulation results were conducted using the BP SX 60 module and a boost converter.

DC-DC boost parameters

Parameters	Values
C_{dc} , mF	$2 \cdot 10^{-4}$
C_{pv} , mF	$3 \cdot 10^{-4}$
L , H	$2 \cdot 10^{-2}$

Tables 2, 3 show the T2FLC membership function of output.

T2FLC parameters

Controller	Parameters	Values
T2FLC	k_1	3
	k_2	4
	k_3	5

T2FLC outputs membership function

ZE	S	M	B
0	0.3	0.7	1

Table 4 presents the T2FLC fuzzy rules, while Figure 5 illustrates the Type-2 fuzzy membership functions for the inputs. Figure 6 depicts the surface of the Type-2 fuzzy logic interval.

Table 4

T2FLC fuzzy rules

de/e	NB	NM	NS	ZE	PS	PM	PB
NB	B	M	S	ZE	S	M	B
NM	B	M	M	S	M	M	B
NS	B	B	M	M	M	B	B
ZE	B	B	B	B	B	B	B
PS	B	B	M	M	M	B	B
PM	B	M	M	S	M	M	B
PB	B	M	S	ZE	S	M	B

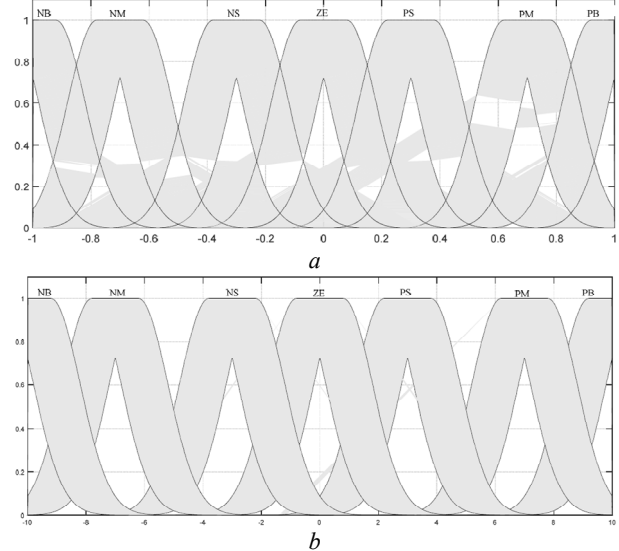


Fig. 5. Type-2 fuzzy function membership of inputs: a – error e ; b – error variation de

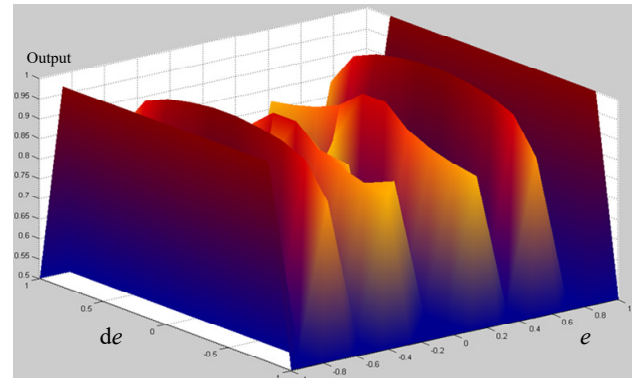


Fig. 6. Surface of the Type-2 fuzzy logic interval

Simulation results are conducted to analyze the effects of different levels of solar irradiation and normal conditions. Figure 7 shows the power and voltage outputs of the PV module under two different steps of irradiation $G = 800 \text{ W/m}^2$ and $G = 1000 \text{ W/m}^2$. The results depicted in Fig. 7 demonstrate that both fuzzy logic approaches (fuzzy Type-2 and fuzzy Type-1) successfully achieve MPP under varying irradiation levels. Specifically, at an irradiation level of 1000 W/m^2 , both methods attain an MPP of 60 W , while at 800 W/m^2 , they achieve an MPP of 48 W . These findings indicate the effectiveness of both fuzzy logic approaches in tracking MPP across different irradiation conditions, ensuring optimal power output.

Figure 8 shows the performance comparison between T2FLC and T1FLC-based MPPT methods, along with the reference voltage V_{ref} . The reference voltage was precisely calculated using a mathematical equation, which dynamically adjusts to these conditions.

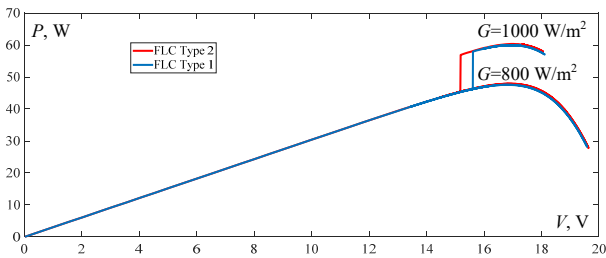


Fig. 7. P - V curves with T1FLC and T2FLC MPPT under two irradiation changes and fixed temperature $T = 25\text{ }^{\circ}\text{C}$

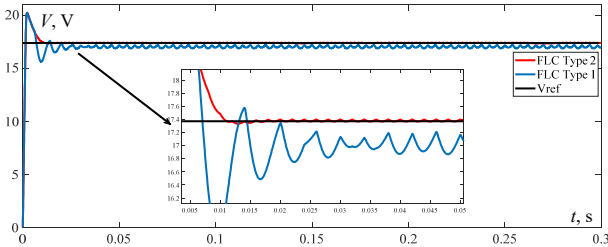


Fig. 8. Output voltage and the voltage reference with T1FLC and T2FLC MPPT under irradiation $G = 1000\text{ W/m}^2$ and $T = 25\text{ }^{\circ}\text{C}$

Figure 9 shows a comparative analysis of T1FLC and T2FLC MPPT in the fixed step of irradiation $G = 1000\text{ W/m}^2$ and temperature $T = 25\text{ }^{\circ}\text{C}$.

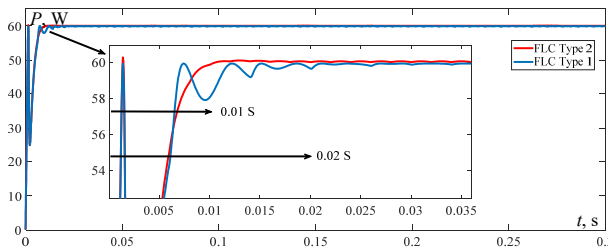


Fig. 9. Output power with T1FLC and T2FLC MPPT under irradiation $G = 1000\text{ W/m}^2$ and $T = 25\text{ }^{\circ}\text{C}$

Figure 10 shows a comparative analysis of T1FLC and T2FLC MPPT in two variations of the steps of irradiation $G = 800\text{ W/m}^2$ and $G = 1000\text{ W/m}^2$ and $T = 25\text{ }^{\circ}\text{C}$. Each change in irradiation level lasted for 0.01 s.

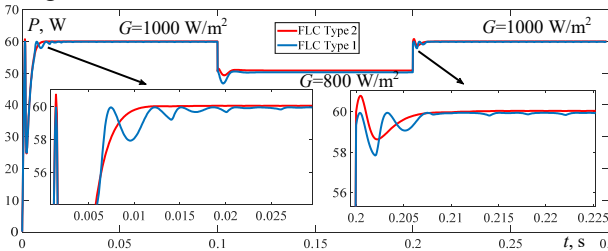


Fig. 10. Output power with T1FLC and T2FLC MPPT under two irradiation changes and fixed temperature $T = 25\text{ }^{\circ}\text{C}$

In Fig. 9, 10 both controllers show an initial surge in power before stabilizing around 60 W. The surge happens quickly, within the first 0.01 s, as both controllers attempt to track the MPP. However, the T2FLC shows a smoother and quicker approach to the MPP compared to the T1FLC. It stabilizes almost 0.01 s before the T1FLC, indicating a faster dynamic response. This is crucial in PV systems, as faster MPPT leads to improved energy efficiency under rapidly changing environmental conditions.

Which remains steady without any oscillations or error, highlighting the effectiveness of the mathematical equation in providing a highly accurate and stable target voltage. This accuracy is crucial for optimal MPPT

performance, as it allows the system to converge to the correct operating point.

T2FLC quickly converges to the reference voltage with minimal oscillations, showcasing its superior performance in tracking the MPP with high precision and stability.

In contrast, the T1FLC exhibits more oscillations around the MPP and a slower convergence to the reference voltage, indicating less precision and stability in comparison to the T2FLC.

The inset zooms in on the initial response period, clearly showing the smooth tracking behavior of the T2FLC and the effectiveness of the reference voltage calculation. The mathematical equation provides a reference voltage that is precise, free from oscillations, and highly reliable, ensuring optimal MPPT performance with no error.

T1FLC exhibits more oscillations during the transient period compared to the T2FLC. These oscillations indicate that the T1FLC is slightly less stable than the T2FLC during the initial phase, which suggests improved stability and reduced power losses due to fluctuations. This could be attributed to the higher flexibility and adaptability of Type-2 fuzzy logic systems, which account for uncertainties better than Type-1 systems.

T2FLC outperforms T1FLC in terms of:

- faster settling time (0.01 s vs. 0.02 s);
- smoother power curve with fewer oscillations.

While both controllers eventually reach a similar steady-state power, the T2FLC demonstrates superior performance, especially in the transient period, which is critical for real-time PV applications where irradiance and temperature can change rapidly.

In summary, T2FLC provides better MPPT performance by reaching the MPP faster and with more stability than T1FLC. This makes it a preferable choice for optimizing PV system efficiency.

Conclusions. The proposed T2FLC-based MPPT system demonstrates significant improvements in the performance of PV systems under dynamic environmental conditions. The enhanced adaptability of the T2FLC, with its ability to manage higher levels of uncertainty through flexible membership functions, allows it to outperform traditional MPPT techniques such as P&O, IC and T1FLCs.

Simulation results validate the achievement of the paper's purpose by showing that the T2FLC-based MPPT system achieves faster response times, reduces power losses caused by oscillations around the MPP, and maintains high accuracy even under rapidly changing irradiance and temperature scenarios. These results confirm the system's ability to optimize energy extraction and improve the overall efficiency and reliability of PV systems.

This research successfully demonstrates the validity of the T2FLC as a robust and efficient control technique for renewable energy applications. By ensuring stable operation and optimizing power output, the T2FLC-based MPPT system offers a promising solution for advancing PV system performance in real-world conditions, thereby fulfilling the objective of enhancing power extraction efficiency under varying environmental conditions.

Conflict of interest. The authors declare that there is no conflict of interest.

REFERENCES

1. Sahraoui H., Mellah H., Drid S., Chrifi-Alaoui L. Adaptive maximum power point tracking using neural networks for a photovoltaic systems according grid. *Electrical Engineering & Electromechanics*, 2021, no. 5, pp. 57-66. doi: <https://doi.org/10.20998/2074-272X.2021.5.08>.

2. Lahiouel Y., Latreche S., Khemliche M., Boulemzaoud L. Photovoltaic fault diagnosis algorithm using fuzzy logic controller based on calculating distortion ratio of values. *Electrical Engineering & Electromechanics*, 2023, no. 4, pp. 40-46. doi: <https://doi.org/10.20998/2074-272X.2023.4.06>.
3. Boudia A., Messalti S., Harrag A., Boukhnifer M. New hybrid photovoltaic system connected to superconducting magnetic energy storage controlled by PID-fuzzy controller. *Energy Conversion and Management*, 2021, vol. 244, art. no. 114435. doi: <https://doi.org/10.1016/j.enconman.2021.114435>.
4. Li X., Wang Q., Wen H., Xiao W. Comprehensive Studies on Operational Principles for Maximum Power Point Tracking in Photovoltaic Systems. *IEEE Access*, 2019, vol. 7, pp. 121407-121420. doi: <https://doi.org/10.1109/ACCESS.2019.2937100>.
5. Assam B., Abderahim Z., Sabir M., Abdelghani H., Boukhnifer M. Modeling and Control Of Grid-PV-SMES System. *2022 International Conference of Advanced Technology in Electronic and Electrical Engineering (ICATEEE)*, 2022, pp. 1-4. doi: <https://doi.org/10.1109/ICATEEE57445.2022.10093729>.
6. Zerzouri N., Ben Si Ali N., Benalia N. A maximum power point tracking of a photovoltaic system connected to a three-phase grid using a variable step size perturb and observe algorithm. *Electrical Engineering & Electromechanics*, 2023, no. 5, pp. 37-46. doi: <https://doi.org/10.20998/2074-272X.2023.5.06>.
7. Mao M., Cui L., Zhang Q., Guo K., Zhou L., Huang H. Classification and summarization of solar photovoltaic MPPT techniques: A review based on traditional and intelligent control strategies. *Energy Reports*, 2020, vol. 6, pp. 1312-1327. doi: <https://doi.org/10.1016/j.egyr.2020.05.013>.
8. Sarvi M., Azadian A. A comprehensive review and classified comparison of MPPT algorithms in PV systems. *Energy Systems*, 2022, vol. 13, no. 2, pp. 281-320. doi: <https://doi.org/10.1007/s12667-021-00427-x>.
9. Sharma A.K., Pachauri R.K., Choudhury S., Minai A.F., Alotaibi M.A., Malik H., Marquez F.P.G. Role of Metaheuristic Approaches for Implementation of Integrated MPPT-PV Systems: A Comprehensive Study. *Mathematics*, 2023, vol. 11, no. 2, art. no. 269. doi: <https://doi.org/10.3390/math11020269>.
10. Gonzalez-Castano C., Restrepo C., Kouro S., Rodriguez J. MPPT Algorithm Based on Artificial Bee Colony for PV System. *IEEE Access*, 2021, vol. 9, pp. 43121-43133. doi: <https://doi.org/10.1109/ACCESS.2021.3066281>.
11. Pathak P.K., Yadav A.K. Design of battery charging circuit through intelligent MPPT using SPV system. *Solar Energy*, 2019, vol. 178, pp. 79-89. doi: <https://doi.org/10.1016/j.solener.2018.12.018>.
12. Al-Majidi S.D., Abbod M.F., Al-Raweshidy H.S. A particle swarm optimisation-trained feedforward neural network for predicting the maximum power point of a photovoltaic array. *Engineering Applications of Artificial Intelligence*, 2020, vol. 92, art. no. 103688. doi: <https://doi.org/10.1016/j.engappai.2020.103688>.
13. Ullah K., Ishaq M., Tchier F., Ahmad H., Ahmad Z. Fuzzy-based maximum power point tracking (MPPT) control system for photovoltaic power generation system. *Results in Engineering*, 2023, vol. 20, art. no. 101466. doi: <https://doi.org/10.1016/j.rineng.2023.101466>.
14. Loukil K., Abbes H., Abid H., Abid M., Toumi A. Design and implementation of reconfigurable MPPT fuzzy controller for photovoltaic systems. *Ain Shams Engineering Journal*, 2020, vol. 11, no. 2, pp. 319-328. doi: <https://doi.org/10.1016/j.asej.2019.10.002>.
15. Muthubalaji S., Devadasu G., Srinivasan S., Soundiraraj N. Development and validation of enhanced fuzzy logic controller and boost converter topologies for a single phase grid system. *Electrical Engineering & Electromechanics*, 2022, no. 5, pp. 60-66. doi: <https://doi.org/10.20998/2074-272X.2022.5.10>.
16. Ali M.N., Mahmoud K., Lehtonen M., Darwish M.M.F. Promising MPPT Methods Combining Metaheuristic, Fuzzy-Logic and ANN Techniques for Grid-Connected Photovoltaic. *Sensors*, 2021, vol. 21, no. 4, art. no. 1244. doi: <https://doi.org/10.3390/s21041244>.
17. Verma P., Garg R., Mahajan P. Asymmetrical interval type-2 fuzzy logic control based MPPT tuning for PV system under partial shading condition. *ISA Transactions*, 2020, vol. 100, pp. 251-263. doi: <https://doi.org/10.1016/j.isatra.2020.01.009>.
18. Abadi I., Uyuniyah Q., Nur Fitriyanah D., Jani Y., Abdullah K. Performance Study of Maximum Power Point Tracking (MPPT) Based on Type-2 Fuzzy Logic Controller on Active Dual Axis Solar Tracker. *E3S Web of Conferences*, 2020, vol. 190, art. no. 00016. doi: <https://doi.org/10.1051/e3sconf/202019000016>.
19. Pratama D.A., Damsi F., Zarkasih M.S. Simulation of Maximum Power Point Tracking with Fuzzy Logic Control Method on Solar Panels Using MATLAB. *Jurnal Teknologi Informasi Dan Pendidikan*, 2024, vol. 17, no. 1, pp. 138-148. doi: <https://doi.org/10.24036/jtip.v17i1.731>.
20. Li I.-H. Design for a Fluidic Muscle Active Suspension Using Parallel-Type Interval Type-2 Fuzzy Sliding Control to improve Ride Comfort. *International Journal of Fuzzy Systems*, 2022, vol. 24, no. 3, pp. 1719-1734. doi: <https://doi.org/10.1007/s40815-021-01229-0>.
21. Rahman A.F.S., Fattah A., Asni A., Waruni M., Kasrani, Ardiansyah W. Fuzzy Logic Control System for Optimizing Dual-Axis Solar Panel Tracking. *E3S Web of Conferences*, 2024, vol. 500, art. no. 03021. doi: <https://doi.org/10.1051/e3sconf/202450003021>.
22. Magaji N., Mustafa M.W. Bin, Lawan A.U., Tukur A., Abdullahi I., Marwan M. Application of Type 2 Fuzzy for Maximum Power Point Tracker for Photovoltaic System. *Processes*, 2022, vol. 10, no. 8, art. no. 1530. doi: <https://doi.org/10.3390/pr10081530>.
23. Kececioğlu O.F., Gani A., Sekkeli M. Design and Hardware Implementation Based on Hybrid Structure for MPPT of PV System Using an Interval Type-2 TSK Fuzzy Logic Controller. *Energies*, 2020, vol. 13, no. 7, art. no. 1842. doi: <https://doi.org/10.3390/en13071842>.
24. Bakkar M., Aboelhasan A., Abdelgelil M., Galea M. PV Systems Control Using Fuzzy Logic Controller Employing Dynamic Safety Margin under Normal and Partial Shading Conditions. *Energies*, 2021, vol. 14, no. 4, art. no. 841. doi: <https://doi.org/10.3390/en14040841>.
25. Merchaoui M., Hamouda M., Sakly A., Mimouni M.F. Fuzzy logic adaptive particle swarm optimisation based MPPT controller for photovoltaic systems. *IET Renewable Power Generation*, 2020, vol. 14, no. 15, pp. 2933-2945. doi: <https://doi.org/10.1049/iet-rpg.2019.1207>.
26. Subramanian V., Indragandhi V., Kuppusamy R., Teekaraman Y. Modeling and Analysis of PV System with Fuzzy Logic MPPT Technique for a DC Microgrid under Variable Atmospheric Conditions. *Electronics*, 2021, vol. 10, no. 20, art. no. 2541. doi: <https://doi.org/10.3390/electronics10202541>.
27. Hong Y.-Y., Buay P.M.P. Robust design of type-2 fuzzy logic-based maximum power point tracking for photovoltaics. *Sustainable Energy Technologies and Assessments*, 2020, vol. 38, art. no. 100669. doi: <https://doi.org/10.1016/j.seta.2020.100669>.
28. Sajan C., Satish Kumar P., Virtic P. Enhancing grid stability and low voltage ride through capability using type 2 fuzzy controlled dynamic voltage restorer. *Electrical Engineering & Electromechanics*, 2024, no. 4, pp. 31-41. doi: <https://doi.org/10.20998/2074-272X.2024.4.04>.
29. Zeghlache S., Djeriou A., Benyetou L., Benslimane T., Mekki H., Bouguerra A. Fault tolerant control for modified quadrotor via adaptive type-2 fuzzy backstepping subject to actuator faults. *ISA Transactions*, 2019, vol. 95, pp. 330-345. doi: <https://doi.org/10.1016/j.isatra.2019.04.034>.
30. Tan W.W., Chua T.W. Uncertain Rule-Based Fuzzy Logic Systems: Introduction and New Directions (Mendel, J.M.; 2001) [book review]. *IEEE Computational Intelligence Magazine*, 2007, vol. 2, no. 1, pp. 72-73. doi: <https://doi.org/10.1109/MCI.2007.357196>.
31. Mendel J.M., John R.I., Liu F. Interval Type-2 Fuzzy Logic Systems Made Simple. *IEEE Transactions on Fuzzy Systems*, 2006, vol. 14, no. 6, pp. 808-821. doi: <https://doi.org/10.1109/TFUZZ.2006.879986>.
32. Qilian Liang, Mendel J.M. Interval type-2 fuzzy logic systems: theory and design. *IEEE Transactions on Fuzzy Systems*, 2000, vol. 8, no. 5, pp. 535-550. doi: <https://doi.org/10.1109/91.873577>.
33. Mendel J.M. On answering the question "Where do I start in order to solve a new problem involving interval type-2 fuzzy sets?" *Information Sciences*, 2009, vol. 179, no. 19, pp. 3418-3431. doi: <https://doi.org/10.1016/j.ins.2009.05.008>.

Received 11.08.2024
Accepted 02.10.2024
Published 02.01.2025

A. Boudia¹, Associate Professor,
S. Messalti¹, Professor,
S. Zeghlache¹, Professor,
A. Harrag², Professor,

¹University of M'sila, Algeria,
e-mail: assam.boudia@univ-msila.dz (Corresponding Author).
²Ferhat Abbas University Setif 1, Algeria.

How to cite this article:

Boudia A., Messalti S., Zeghlache S., Harrag A. Type-2 fuzzy logic controller-based maximum power point tracking for photovoltaic system. *Electrical Engineering & Electromechanics*, 2025, no. 1, pp. 16-22. doi: <https://doi.org/10.20998/2074-272X.2025.1.03>